

Study of Bond Angles and Bond Lengths in Disiloxane and Related Molecules in Terms of the Topology of the Electron Density and Its Laplacian

Ronald J. Gillespie* and Samuel A. Johnson

Department of Chemistry, McMaster University, Hamilton, Ontario, L8S 4M1 Canada

Received November 18, 1996[⊗]

We have calculated the electron density distributions for the series of molecules H_nXOXH_n , $X = Li$ to F and Na to Cl , and some related molecules. We have analyzed these distributions and their Laplacian to obtain atomic charges, electron densities at the bond critical point, and the charge concentrations revealed by the Laplacian. On the basis of this information and an analysis of the $X-O$ bond lengths and angles, we have examined the factors that determine the lengths of the $X-O$ bonds and the XOX bond angles. The XO bond length reaches a minimum value at boron in period 2 and at silicon in period 3 when the product of the charges on X and O reaches a maximum value, consistent with a predominately ionic model for the molecules $X = Li, Be, B, Na, Mg, Al,$ and Si . In the remaining molecules of both series, the XO bonds have an increasing covalent character. The bond length and the bond angle in disiloxane are consistent with the ionic character of the molecule, and there is no evidence for the frequently quoted back-bonding model. In disiloxane and related molecules in which the ligand is considerably less electronegative than oxygen the electrons in the valence shell of oxygen are not well localized into pairs, so the bond angle is intermediate between the tetrahedral angle expected when the valence shell electrons of oxygen are strongly localized into four tetrahedral pairs and the 180° bond angle expected on the basis of the electrostatic and/or steric repulsion between the positively charged X atoms. The effects on the bond lengths and angles of substituting oxygen by sulfur and hydrogen by fluorine are discussed.

Introduction

According to the VSEPR model,^{1–3} AX_2E_2 molecules are expected to have an angular shape with a bond angle equal to or slightly less than the tetrahedral angle of 109.5° , depending on the electronegativity of the ligand. Although some AX_2E_2 molecules in which the central atom is oxygen, such as H_2O (104.4°), F_2O (103.1°), FOH (97.2°), and $HOOH$ (94.8°), have angles that are in accord with this prediction some OX_2E_2 molecules have bond angles that are larger than the tetrahedral angle. A much discussed example is disiloxane, $H_3SiOSiH_3$, which has a bond angle of 144.1° .⁴ Not only is the bond angle in disiloxane large, but the barrier to linearization is very small ($0.32 \text{ kcal mol}^{-1}$).^{4,5}

The large bond angle in disiloxane has commonly been attributed to delocalization of oxygen lone pair electrons from the filled valence shell of oxygen into the incompletely filled valence shell of silicon, in other words, in terms of the atomic orbital model, into vacant 3d orbitals on silicon, forming (p-d) π bonds in what is described as back-bonding.^{4,6–13} The SiO bonds are thus considered to have some double bond character,

and, in terms of the VSEPR model, the correspondingly increased size of the SiO bond domains and the decreased size of the nonbonding domains are responsible for the large bond angle.² That the SiO bonds in $H_3SiOSiH_3$ are considerably shorter (163.4 pm)⁴ than the sum of the single bond covalent radii ($191–193 \text{ pm}$)¹⁴ is also consistent with the SiO bonds having some double bond character. However, several authors have subsequently shown from an analysis of ab initio calculations that d orbitals do not play a significant role in the Si–O bond,^{15–17} although the (p-d) π back-bonding model is often still described in textbooks.¹⁸ Several alternative explanations have, therefore, been proposed. For example, in a modified form of the back-bonding model, it has been suggested that oxygen lone pair electrons are donated into Si–H σ^* orbitals rather than into Si 3d orbitals.^{15,17} Alternatively, Oberhammer and Boggs¹⁶ proposed that the Si–O bond is strongly ionic and that this is the principal cause of the apparently short bonds. In a recent paper discussing the lengths of bonds to fluorine,¹⁹ including the Si–F bond, we have shown that they are predominately ionic and that they only appear to be short because they are unjustifiably compared to the sum of the covalent radii. Because oxygen is second only to fluorine in electronegativity, we expect the Si–O bond to also be strongly

[⊗] Abstract published in *Advance ACS Abstracts*, June 1, 1997.

- (1) Gillespie, R. J.; Robinson, E. A. *Angew. Chem., Int. Ed. Engl.* **1996**, *35*, 495.
- (2) Gillespie, R. J.; Hargittai, I. *The VSEPR Model of Molecular Geometry*; Allyn and Bacon: Boston, 1991.
- (3) Gillespie, R. J. *Chem. Soc. Rev.* **1992**, 59.
- (4) Allmenningen, A.; Bastiensen, O.; Ewing, V.; Hedberg, K.; Traetteberg, M. *Acta Chem. Scand.* **1963**, *17*, 2455.
- (5) Durig, J. R.; Flanagan, M. J.; Kalinsky, V. F. *J. Chem. Phys.* **1977**, *66*, 2775.
- (6) Voronkov, M. G.; Mileshkevish, V. P.; Yuzhelevskii, Y. A. *The Siloxane Bond*; Consultants Bureau: New York, 1978.
- (7) Glidewell, C.; Rankin, D. W. H.; Robirette, A. G.; Sheldrick, G. M.; Beagly, B.; Freeman, J. M. *J. Mol. Struct.* **1970**, *5*, 417.
- (8) Blake, A. J.; Ebsworth, E. A. V.; Henderson, S. G. D.; Dysrbuch, M. *Acta Crystallogr.* **1988**, *C44*, 1.
- (9) Ernst, C. A.; Allred, A. L.; Raytner, M. A.; Newton, M. D.; Gibbs, G. V.; Moskowitz, J. W.; Topiol, S. *Chem. Phys. Lett.* **1981**, *81*, 424.
- (10) Allmenningen, A.; Hedberg, K.; Seip, R. *Acta Chem. Scand.* **1963**, *17*, 2264.

- (11) Varma, R.; MacDiarmid, A. G.; Miller, G. *Inorg. Chem.* **1964**, *3*, 1754.
- (12) Ebsworth, E. A. V. In *Organometallic Compounds of the Group IV Elements*; MacDiarmid, A. G., Ed.; Marcel Dekker: New York, 1968.
- (13) Burger, H. *Angew. Chem.* **1973**, *85*, 519.
- (14) Values for the covalent radius of oxygen ranging from 74 to 65 pm have been proposed, as has been discussed in detail in ref 19. The covalent radius of silicon is 117 pm (ref 2).
- (15) Luke, B. T.; Pople, J. A.; Krogh-Jespersen, B.; Apeloig, Y.; Chandrasekhar, J.; Schleyer, P. v. R. *J. Am. Chem. Soc.* **1986**, *108*, 260.
- (16) Oberhammer, H.; Boggs, J. E. *J. Am. Chem. Soc.* **1980**, *102*, 7241.
- (17) Shambayati, S.; Blake, J. F.; Wierschke, S. G.; Jorgensen, W. L.; Schreiber, S. L. *J. Am. Chem. Soc.* **1990**, *112*, 697.
- (18) See, for example: Alcock, N. *Bonding and Structure*; Ellis Horwood: London, 1990; p 228.
- (19) Robinson, E. A.; Johnson, S. A.; Tang, T.-H.; Gillespie, R. J. *Inorg. Chem.* **1997**, *36*, 3022.

Table 1. Geometry and Energies for the Molecules $(H_nX)_2O$, $(F_nX)_2O$, and $(H_nX)_2S^a$

molecule	bond lengths (pm)		X—O—X bond angle (deg)	-E (au)	linearization energy (kcal mol ⁻¹)
	X—O	X—H (X—F)			
Li ₂ O	159.6 (160)		180.0 (180)	89.806710	0
(HBe) ₂ O	139.6	133.2	180.0	105.457703	0
(H ₂ B) ₂ O	135.4	119.0	126.9	126.662912	1.9
(H ₃ C) ₂ O	139.0 (141.0)	108.4 (109.6)	113.9 (111.7)	154.120200	36
(H ₃ N) ₂ O	138.9	99.9	109.8	186.024898	74.9
(HO) ₂ O	136.5	94.5	107.8	225.446479	113.6
F ₂ O	133.6 (140.5)		103.5 (103.1)	273.550435	156.9
F ₂ O ^b	140.5		104.0	274.759987	
Na ₂ O	197.3		180.0	398.534504	0
(HMg) ₂ O	178.2	170.5	180.0	475.318544	0
(H ₂ Al) ₂ O	167.1	157.5	180.0	561.162672	0
(H ₃ Si) ₂ O	162.1 (163.4)	147.2 (148.6)	148.3 (144.1)	656.349671	0.4
(H ₂ P) ₂ O	163.6	140.9	129.8	758.711594	11.2
(HS) ₂ O	165.4	132.8	119.1	871.010318	30.7
Cl ₂ O	166.5 (169.6)		112.8 (111.2)	993.661248	56.9
(F ₃ C) ₂ O	135.4 (136.9)	129.8 (132.7)	118.9	747.505487	
(F ₃ Si) ₂ O	158.3 (158.1)	154.4 (155.4)	162.2 (156)	1250.162856	
(H ₃ Ge) ₂ O	175.2 (176.6)	156.6 (153.1)	138.2 (126.5)	4229.057624	
(H ₃ C) ₂ S	180.9 (180.7)	108.0 (111.6)	100.4 (99.1)	476.791361	
(H ₃ Si) ₂ S	215.8 (212.9)	146.8 (149.2)	102.1 (98.4)	978.965886	

^a Experimental data in parentheses. References: Li₂O, ref 15; (CH₃)₂O, Blakis, V.; Kasa, P. H.; Myers, R. J. *J. Chem. Phys.* **1963**, *38*, 2753; (H₃Si)₂O, ref 4; Cl₂O, Beagely, B.; Clark, A. H.; Hewitt, T. G. *J. Chem. Soc. (A)* **1968**, 658; (F₃C)₂O, Lowrey, A. H.; George, C.; D'Antonio, P. *J. Mol. Struct.* **1980**, *62*, 243; (F₃Si)₂O, Airey, W.; Glidewell, C.; Rankin, D. W. H.; Robiette, A. G.; Sheldrick, G. M.; Cruickshank, D. W. J. *Trans. Faraday Soc.* **1970**, *66*, 551; (H₃Ge)₂O, Glidewell, C.; Rankin, D. W. H.; Robiette, A. G.; Sheldrick, G. M.; Beagely, B.; Ceadoxk, S. J. *Chem. Soc. (A)* **1970**, 315; (H₃C)₂S, Tijjima, T.; Tsuchiya, S.; Kimura, M. *Bull. Chem. Soc. Jpn.* **1977**, *50*, 2564; (H₃Si)₂S, Dossel, K. F. *Z. Naturforsch.* **1978**, *33a*, 1190. ^b B3/LYP calculation. See ref 19.

ionic, as we confirm in this paper, and as previously suggested by Oberhammer and Boggs.¹⁶ These authors proposed that the large bond angle is principally due to steric and electrostatic repulsions between the SiH₃ groups. Glidewell²⁰ has also attributed the large bond angle to steric effects. However, the steric argument clearly cannot apply to the very ionic Li₂O molecule, which is linear.²¹ This molecule is usually regarded as having ionic bonding, and its linear geometry is attributed to electrostatic repulsion between the two Li⁺ ions.

It is noteworthy that the SiO bond in the various forms of SiO₂ is also very short, with a length of 163 pm in β -cristobalite and β -trydimite and a corresponding SiOSi bond angle of 144°. The bonding in silica is usually regarded as having considerable ionic character, and back-bonding has not usually been invoked in the discussion of these bond lengths and angles.

The object of the present work was to attempt to improve our understanding of the factors influencing the bond angles and bond lengths in OX₂E₂ molecules by using an approach based on the analysis of electron distributions calculated by ab initio methods. We have calculated the bond lengths, bond angles, and electron density distributions and analyzed the electron density distribution in terms of its Laplacian^{23,24} for the following molecules: Li₂O, (BeH)₂O, (BH₂)₂O, (CH₃)₂O, (NH₂)₂O, (HO)₂O, and F₂O; Na₂O, (MgH)₂O, (AlH₂)₂O, (SiH₃)₂O, (PH₂)₂O, (SH)₂O, and Cl₂O; and (CF₃)₂O, (SiF₃)₂O, (CH₃)₂S, (SiH₃)₂S, and (GeH₃)₂O.

Calculations

All the wave functions for the molecules studied using the Gaussian 92 package,²⁵ with the exception of (H₃Ge)₂O, for which Gaussian 94 was used.²⁶ All the calculations were performed at the Hartree-Fock (HF) level of theory using the basis set 6-311++G(2d,2p) with 6d functions. The analysis of these wave functions was carried out using the AIMPAC suite of programs.²⁷ The molecules were assumed to have at least a C₂ axis of symmetry. Additionally, (H₃Si)₂O, (H₃C)₂O, (H₂P)₂O, (CF₃)₂O, (SiF₃)₂O, (CH₃)₂S, (SiH₃)₂S, and (GeH₃)₂O were assumed to have C_{2v} symmetry. In those cases in which the optimized geometry of the H_nXOX_n molecules is angular, calculations were also performed with the geometry constrained to be linear. For these

calculations, the following minimum symmetries are assumed: D_{3h}, (SiH₃)₂O, (CH₃)₂O; C_{2v}, (H₂N)₂O, (H₂P)₂O; C₂, all others.

It is well known that, in order to obtain satisfactory geometrical parameters and atomic charges for molecules such as F₂, O₂, F₂O, and HOF,^{28,29} it is necessary to include electron correlation by doing MP2 or DFT calculations such as B3LYP³⁰ rather than HF calculations. For F₂O, therefore, we use the results of B3LYP calculations given in ref 19.

Results and Discussion

Geometry. The optimized geometry and the energy for each of the molecules studied are given in Table 1. Our results for H₂BOBH₂ are in good agreement with a recent ab initio study of this molecule at the HF and MP2 levels,³¹ which gave the

- (20) Glidewell, C. *Inorg. Chim. Acta* **1975**, *12*, 219.
- (21) White, D.; Seshadri, K. S.; Dever, D. F.; Mann, D. E.; Linevsky, M. J. *J. Chem. Phys.* **1963**, *39*, 2299. Buchler, A.; Stauffer, F. L.; Klemperer, W.; Wharton, L. *J. Chem. Phys.* **1963**, *39*, 2463.
- (22) Wells, A. F. *Structural Inorganic Chemistry*, 4th ed.; Clarendon Press: Oxford, 1975; p 805.
- (23) Bader, R. F. W. *Atoms in Molecules: A Quantum Theory*; Clarendon Press: Oxford, 1990.
- (24) Bader, R. F. W.; McDougall, P. J.; Lau, C. D. H. *J. Am. Chem. Soc.* **1984**, *106*, 1594.
- (25) Frisch, M. J.; Trucks, G. W.; Head-Gordon, M.; Gill, P. M. W.; Wong, M. W.; Foresman, J. B.; Johnson, B. G.; Schlegel, H. B.; Robb, M. A.; Replogle, E. S.; Gomperts, R.; Andres, J. L.; Raghavachari, K.; Binkley, J. S.; Gonzalez, C.; Martin, R. L.; Fox, D. J.; Defrees, D. J.; Baker, J.; Stewart, J. P. *Gaussian 92*; Gaussian, Inc.: Pittsburgh, PA, 1992.
- (26) Frisch, M. J.; Trucks, G. W.; Schlegel, H. B.; Gill, P. M. W.; Johnson, B. G.; Robb, M. A.; Cheeseman, J. R.; Keith, T.; Petersson, G. A.; Montgomery, J. A.; Raghavachari, K.; Al-Laham, M. A.; Zakrzewski, V. G.; Ortiz, J. V.; Foresman, J. B.; Peng, C. Y.; Avalla, P. Y.; Chen, W.; Wong, M. W.; Andres, J. L.; Replogle, E. S.; Gomperts, R.; Martin, R. L.; Fox, D. J.; Binkley, J. S.; Defrees, D. J.; Stewart, J. P.; Head-Gordon, M.; Gonzalez, C.; Pople, J. A. *Gaussian 94, Revision B.3*; Gaussian Inc.: Pittsburgh, PA, 1995.
- (27) Biegler-König, F. W.; Bader, R. F. W.; Tang, T.-H. *J. Comput. Chem.* **1982**, *3*, 317.
- (28) Valenta, K. E.; Vasudevan, K.; Grein, F. *J. Chem. Phys.* **1980**, *72*, 2148.
- (29) Wang, J.; Eriksson, L. A.; Johnson, B. G.; Boyd, R. J. *J. Phys. Chem.* **1996**, *100*, 5274.
- (30) Becke, A. *J. Chem. Phys.* **1993**, *98*, 5648.

following values: B–O, 135.7 pm (HF), 137.6 pm (MP2); B–H, 119.1 pm (HF), 119.2 pm (MP2); \angle BOB, 125.3° (HF), 123.0° (MP2).

For the period of 2 (H_nX)₂O molecules, the XOX bond angle decreases steadily from 180° to less than the tetrahedral angle, and for the period 3 molecules, it decrease from 180° to slightly larger than the tetrahedral angle. The SiOSi and COC angles are both consistent with the general trend of bond angles in the two series, and, in particular, the SiOSi bond angle does not appear to be anomalous. The expected VSEPR angle ($<109.6^\circ$) is found only when X is either of the very electronegative groups OH or F. The energy of linearization (Table 1) increases steadily from zero for the linear molecules through very low values for (H_2B)₂O and (H_3Si)₂O, indicating that these are very “floppy” molecules, to relatively large values for the remaining molecules, which become increasingly difficult to bend.

Electron Density Distributions. The electron density distributions are illustrated by contour diagrams of the electron density in the XOX plane for a selection of the molecules studied (Figure 1). In each case, there is a local maximum at each nucleus. At such a maximum, all three curvatures in the electron density, $\partial^2\rho/dx^2$, $\partial^2\rho/dy^2$, and $\partial^2\rho/dz^2$, are negative, and this point is described as a (3, -3) critical point because there are three nonzero curvatures and the sum of their signs is -3.²³ Pairs of nuclei that are considered to be bonded together are joined by a line called a *bond path*, along which the electron density is greater than that in any direction perpendicular to the bond path. The point of minimum electron density along a bond path is called the *bond critical point*. This point is a saddle point, that is, a (3, -1) critical point at which there are three nonzero curvatures, of which two are negative and one is positive, so that the sum of their signs is -1. There is a *zero-flux surface* separating each atom from its neighbors.²³ These zero-flux surfaces serve to define the atom in the molecule, and by integrating the electron density over the regions defined by these interatomic surfaces, the *charge* on each atom can be found. In a contour map of the electron density in a plane, such as those shown in Figure 1, we see the lines along which a zero-flux surface cuts the plane.

The atomic charges, $q(X)$, and the electron density at the bond critical point, ρ_b , for all the molecules are given in Table 2. The negative charge on oxygen decreases steadily from Li₂O to (HO)₂O and becomes positive in F₂O; it decreases from Na₂O to Cl₂O, indicating an increasing covalent character to the bonds in both series, except for the increase in polarity in the reverse sense in F₂O. The charge on oxygen shows a good correlation with the electronegativity of the attached atom (Figure 2), and the form of the relationship is remarkably similar to that between the charge on fluorine and the electronegativity of the attached atom in the period 2 and 3 fluorides.¹⁹ The charge on X increases to a maximum at boron in period 2 and at silicon in period 3. The product of the charges on X and O similarly reaches a maximum at boron and silicon. In the very ionic molecules such as (HBe)₂O, the contours of ρ (Figure 1) surrounding the oxygen and the X atoms are almost spherical, with only a contour of very low value surrounding both nuclei, indicating that there is very little shared density, as is also clear from the small values of ρ_b . In (H_2B)₂O, the increased distortion of the oxygen valence shell electron density as it becomes increasingly shared is shown by the stretching out of the contours in the bond direction and by the increased value of ρ_b . These changes in ρ continue in (CH_3)₂O, where a slight “bulging out” of the contours in the expected direction of lone

pair electron density can also be seen. The shape of these contours indicates that the electron density is decreasing less rapidly in this direction than in other directions, as it also does along the bond paths. The increase in ρ_b and the increasing covalent character of the bonding seen in the contour maps continue in the remaining molecules of this series. Moreover, the bulging out of the contours, indicating a less rapid decrease in ρ in the lone pair directions, becomes even more prominent both on the oxygen atom and on the ligands. The same trends are observed in the series Na₂O to Cl₂O, although it is not until (H_3Si)₂O that any significant distortion of the oxygen contours from spherical is observed, consistent with the greater ionic character of the period 3 molecules.

Bond Lengths. On the basis of either ionic radii or covalent radii, we would expect a continuous decrease in bond length across each period. But we see from Table 1 and Figure 3 that the X–O bond length decreases to a minimum value at boron in period 2 and at silicon in period 3. In period 2, the bond length then increases up to carbon and nitrogen, after which it remains essentially constant, as shown by the calculated (B3/LYP) and experimental values for F₂O. In period 3, the bond length increases slowly from Si to Cl. It is striking that the minimum bond length occurs when the product of the charges on X and O reaches a maximum in both periods. In our recent paper on X–F bond lengths,¹⁹ we reported a very similar dependence of the bond lengths in the period 2 and 3 fluorides on the product of the charges on X and F. We attribute this dependence of bond length on the product of the atomic charges to the electrostatic attraction between the oppositely charged atoms, which reaches a maximum at boron and silicon. Consistent with this interpretation, we note that the average bond energy values for B–O (536 kJ mol⁻¹) and Si–O (452 kJ mol⁻¹), and the bond energies for the corresponding bonds to fluorine, B–F (613 kJ mol⁻¹) and Si–F (565 kJ mol⁻¹),³² show that these are among the strongest known single bonds. In period 3, except for ClF, the calculated and observed bond lengths are smaller than the sum of the covalent radii because of the ionic contribution to the bonding. In period 2, this is also the case up to carbon. For the more covalent molecules, the O–X bond length remains almost constant or decreases only slightly, in contrast to the decrease expected from the sum of the covalent radii.³⁴ A similar behavior is observed for the bond lengths in the period 2 fluorides.¹⁹

It might have been expected that the bond lengths for the first very ionic members of both series would agree well with the sum of the ionic radii. However, although the lengths obtained from the sum of the ionic radii given by Shannon³³ decrease as expected across each group, they are larger than the calculated or observed values, except for B and Si. This is because the radii that we used are for the smallest coordination number given by Shannon, which is usually four, whereas in the isolated molecules it is only 1 for Li and Na, 2 for Be and Mg, and 3 for B and Al.

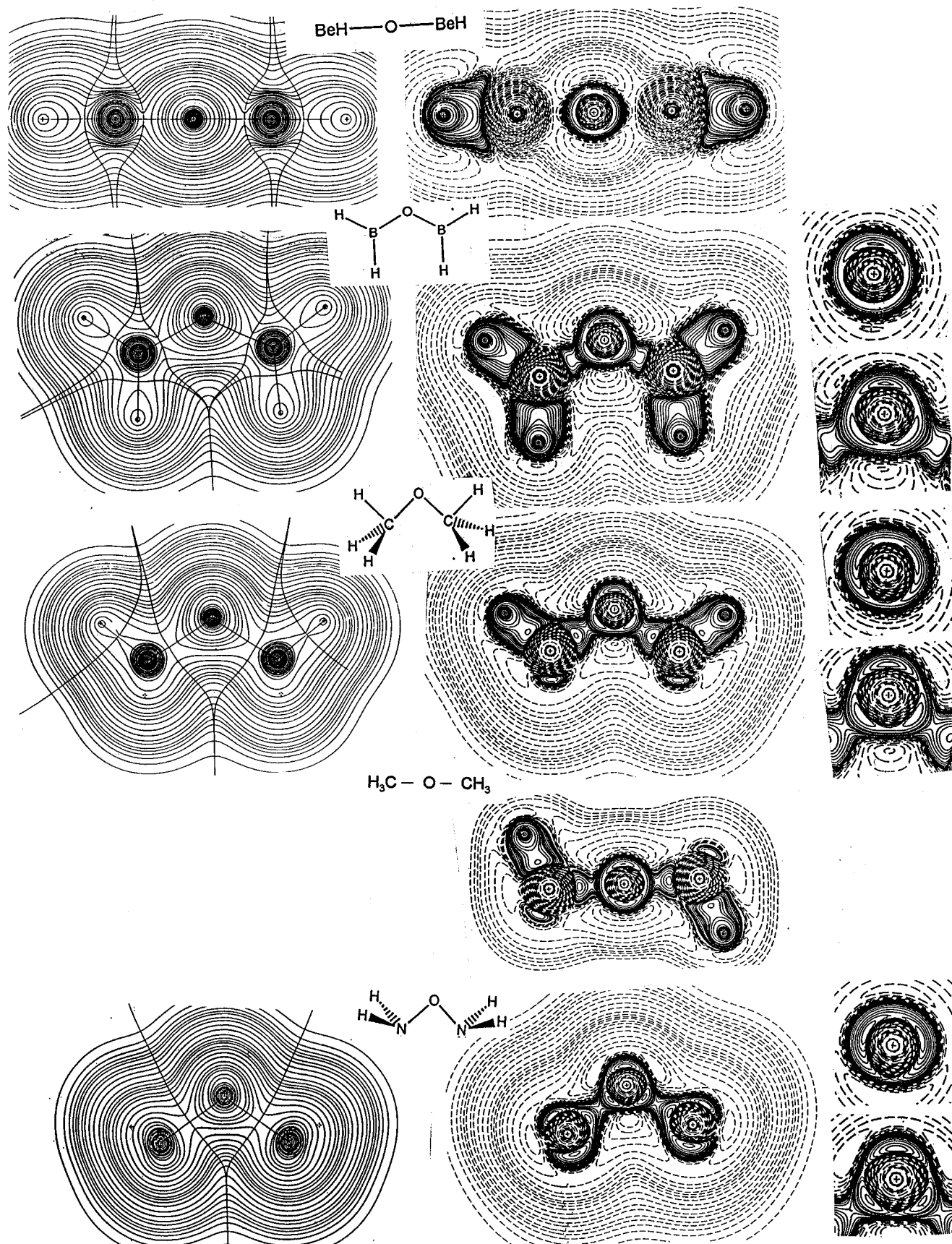
Bond Angles in the H_nXOXH_n Molecules and the Laplacian of the Electron Density. Our results show that, for the H_nXOXH_n series of molecules, only the predominately covalent molecules with the most electronegative ligands, namely F₂O, (HO)₂O, and (H₂N)₂O, have bond angles that are smaller than 109.5° as predicted by the VSEPR model, while the bond angle

(31) Gatti, F.; Berthe-Gaujac, N.; Demachy, I.; Volatron, F. *Chem. Phys. Lett.* **1995**, *232*, 503.

(32) Huheey, J. E.; Keiter, E. A.; Keiter, R. L. *Inorganic Chemistry*, 4th ed.; Harper Collins: New York, 1993.

(33) Shannon, R. D. *Acta Crystallogr.* **1976**, *A32*, 751.

(34) Covalent radii were standard values (see ref 2), and values of 65 pm for O and 60 pm for F were used (see ref 19).



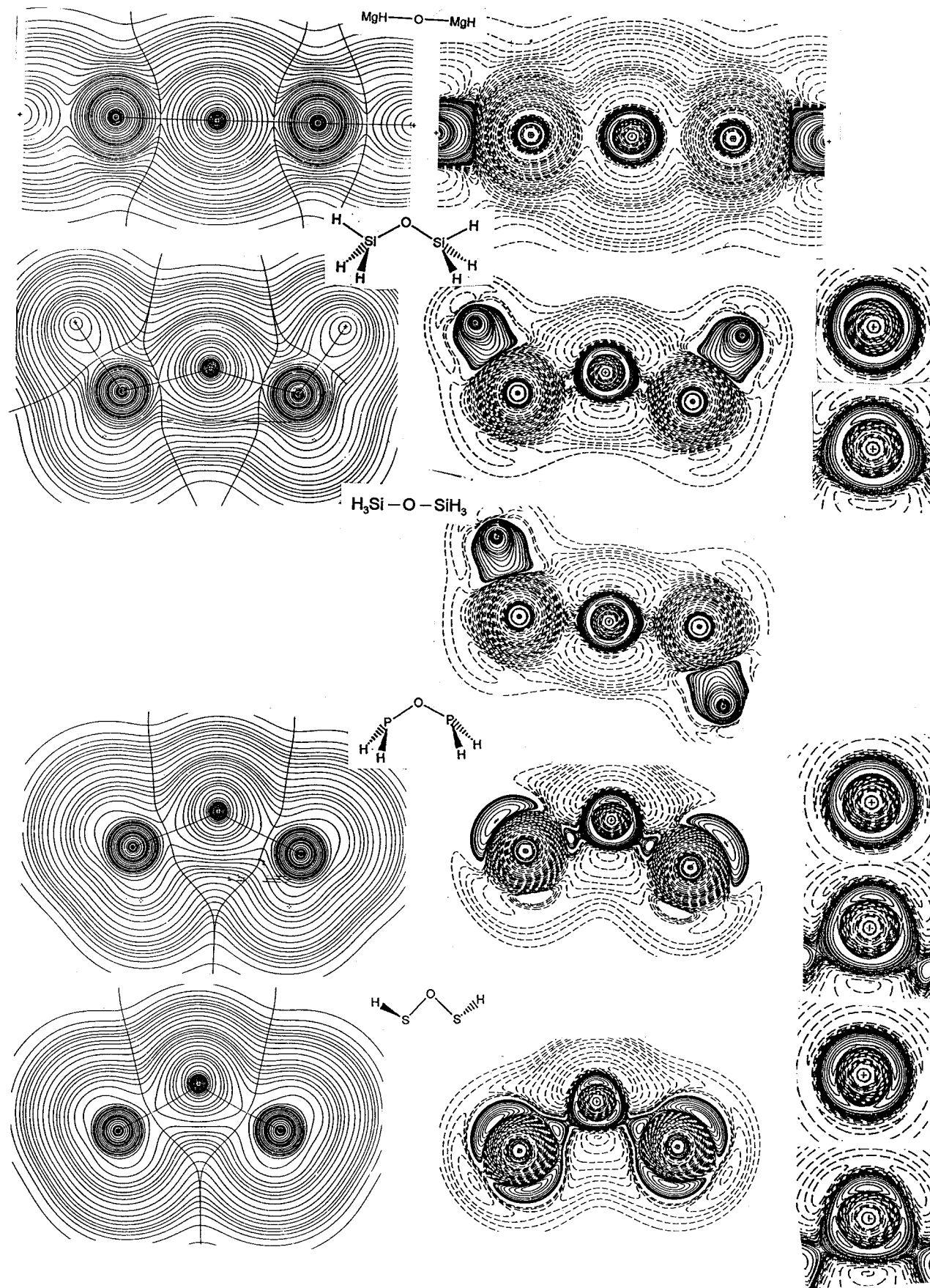
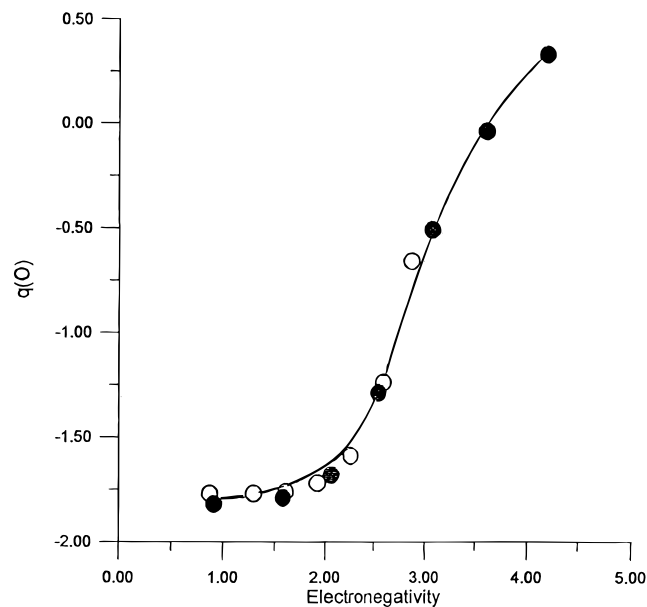


Figure 1. Left column: electron density contour maps. Middle column: Laplacian contour maps. Right column: enlargement of the Laplacian of the oxygen atom for the angular molecules (upper, plane perpendicular to XOX plane; lower, XOX plane). The contours in these plots have the values $1, 2, 3, 4, 5, 6,$ and 8×10^{-n} ($n = -3$ and $+2$) and $1, 1.4, 2, 3, 4, 5, 6,$ and 8×10^{-n} ($n = -2, -1, 0, +1$). Negative values of L are shown by dashed lines.

Table 2. Electron Density at the X–O Bond Critical Point, ρ_b , and Atomic Charges for $(H_nX)_2O$, $(F_3X)_2O$, and $(H_3X)_2S$ Molecules

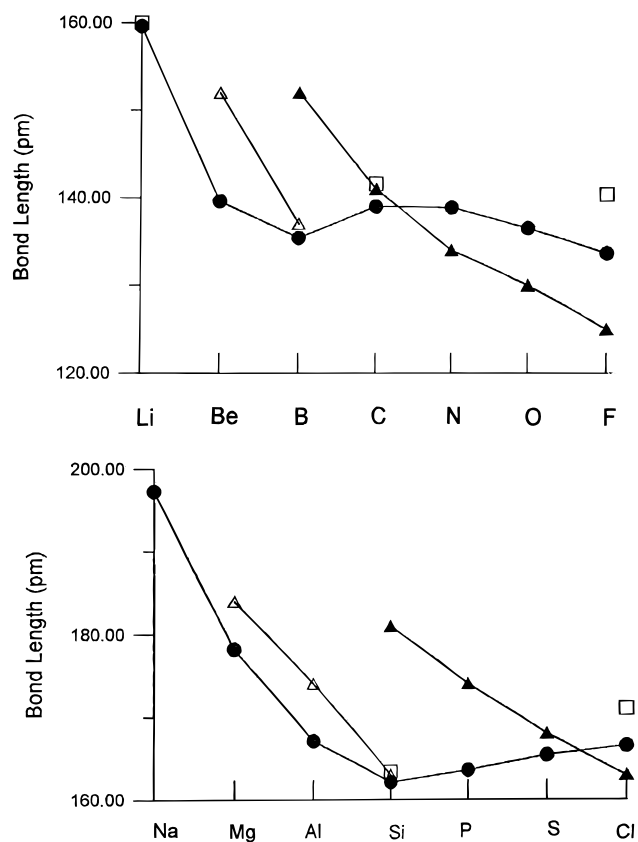
molecule	ρ_b (au)	$q(O)$ or $q(S)$	$q(X)$	$q(O)q(X)$	$q(H)$ or $q(F)$
Li_2O	0.080	-1.82	+0.91	-1.65	
$(HBe)_2O$	0.148	-1.79	+1.74	-3.11	-0.85
$(H_2B)_2O$	0.209	-1.68	+2.27	-3.81	-0.72
$(H_3C)_2O$	0.273	-1.29	+0.78	-1.01	-0.05
$(H_2N)_2O$	0.329	-0.51	-0.46	+0.23	+0.36
$(HO)_2O$	0.357	-0.04	-0.62	+0.02	+0.64
F_2O	0.370	+0.33	-0.17	+0.06	
F_2O^a	0.295	+0.28	-0.13	-0.04	
Na_2O	0.053	-1.77	+0.88	-1.56	
$(HMg)_2O$	0.082	-1.77	+1.69	-2.99	-0.81
$(H_2Al)_2O$	0.113	-1.76	+2.45	-4.29	-0.78
$(H_3Si)_2O$	0.141	-1.72	+3.05	-5.25	-0.73
$(H_2P)_2O$	0.161	-1.59	+1.97	-3.13	-0.59
$(HS)_2O$	0.190	-1.24	+0.75	-0.93	-0.13
Cl_2O	0.214	-0.66	+0.33	-0.22	
$(CF_3)_2O$	0.317	-1.32	+2.84	-3.75	-0.74
$(F_3Si)_2O$	0.156	-1.68	+3.13	-5.26	-0.96
$(H_3Ge)_2O$	0.144	-1.56	+2.11	-3.29	-0.46
$(H_3C)_2S$	0.182	+0.03	+0.03	0.00	-0.01
$(H_3Si)_2S$	0.094	-1.47	+2.90	4.26	-0.72

^a B3/LYP calculation. See ref 19.

**Figure 2.** Plot of the charge on oxygen against the electronegativity of X.

increases with decreasing electronegativity of the ligand up to the limiting value of 180° for the most ionic molecules, such as Li_2O .

According to the VSEPR model, bond angles of 109° or less at oxygen are due to the presence of nonbonding electron pairs in the valence shell of the oxygen atom. However, the electron density distributions give little evidence for these nonbonding electrons, although an increasing deviation from a spherical electron density distribution in the direction of the expected lone pairs on the oxygen atom, as shown by the bulging out of the electron density contours in the lone pair directions in the more covalent molecules, gives a hint of their presence. Moreover, even the shell structure of each atom is not evident in the total electron density. We therefore analyzed the electron density distribution of each molecule in terms of its Laplacian, $L = -\nabla^2\rho$, because it has been shown that the electron shells and bonding and lone pairs of electrons are clearly revealed as regions of charge concentration.^{23,35} In particular, the electron shells are revealed as spherical regions of charge concentration in which L has a positive value, separated by regions of charge

**Figure 3.** XO bond lengths for the $(H_nX)_2O$ molecules of periods 2 and 3: ●, calculated bond lengths; ▲, sum of the covalent radii; △, sum of the ionic radii; □, experimental values (also for X = F the B3/LYP calculated value). Top, period 2; bottom, period 3.

depletion in which L has a negative value. In molecules, the spherical region of charge concentration corresponding to the valence shell is distorted to give local maxima or $(3, -3)$ critical points³⁶ in the topology of L that in many molecules correspond to the number and positions of the lone pairs and bonding pairs predicted by the VSEPR model.³⁵ These charge concentrations (CCs) are accordingly referred to as bonding CCs and lone pair CCs. They are separated by $(3, -1)$ critical points or saddle points in the topology of L .

Contour maps of L in the XOX plane for a selection of the H_nXOXH_n molecule studied are given in Figure 1, and the results of the analysis of L for all the molecules are given in Table 3. In the plot for dimethyl ether, there are four charge concentrations in the valence shell of oxygen. Two of them are along the C–O bond paths and may be called bonding charge concentrations (bonding CCs). The other two are in the plane through the oxygen nucleus and perpendicular to the molecular plane and are nonbonding CCs, giving a nearly tetrahedral arrangement of four CCs, corresponding to the four approximately tetrahedral electron pair domains of the VSEPR model. For the more electronegative ligands NH_2 , OH , and F in period 2 and for SH and Cl in period 3, two bonding and two nonbonding CCs with a tetrahedral arrangement are similarly observed. However, for ligands that are less electronegative than carbon, only a single nonbonding CC on oxygen is found for BH_2 , SiH_3 , and PH_2 and none for the most weakly

(35) Bader, R. F. W.; Gillespie, R. J.; MacDougall, P. J. *J. Am. Chem. Soc.* **1988**, *110*, 7320.

(36) In the more covalent molecules, the bonding CCs appear as $(3, -1)$ critical points because one of the three curvatures in L has a small positive value. However, in Figure 1, these $(3, -1)$ critical points appear as maxima because the small positive curvature is in the direction perpendicular to the molecular plane.

Table 3. Properties of the Laplacian of the Oxygen Atom in the Optimized Molecules^a

molecule	bonding charge concentrations				nonbonding charge concentrations			
	critical points	<i>L</i>	<i>r</i> (cc-O) (pm)	angles (deg)	critical points	<i>L</i>	<i>r</i> (cc-O) (pm)	angle (deg)
Li ₂ O	2(3, -3)	4.271	35.3	180				
(HBe) ₂ O	2(3, -3)	3.745	36.1	180				
(H ₂ B) ₂ O	2(3, -3)	3.896	36.5	109	1(3, -3)	5.290	34.3	
(H ₃ C) ₂ O	2(3, -3)	2.706	37.4	104	2(3, -3)	5.688	34.2	128
(H ₂ N) ₂ O	2(3, -1)	2.196	38.8	103	2(3, -3)	6.887	33.5	142
(HO) ₂ O	2(3, -1)	1.707	39.6	101	2(3, -3)	8.470	32.8	152
F ₂ O	2(3, -1)	1.256	40.4	100	2(3, -3)	10.02	32.1	155
Na ₂ O	2(3, -3)	3.601	35.7	180				
(HMg) ₂ O	2(3, -3)	3.522	36.0	180				
(H ₂ Al) ₂ O	2(3, -3)	3.348	36.4	180				
(H ₃ Si) ₂ O	2(3, -3)	3.072	36.8	112	1(3, -3)	3.812	35.3	
(H ₂ P) ₂ O	2(3, -3)	2.841	37.3	105	1(3, -3)	4.750	34.6	
(HS) ₂ O	2(3, -1)	2.270	38.2	102	2(3, -3)	5.667	34.1	125
Cl ₂ O	2(3, -1)	1.650	39.2	100	2(3, -3)	7.318	33.1	151

^a $L = -\nabla^2\rho$ in atomic units, $r(\text{cc-O})$ is the distance from the charge concentration to the oxygen nucleus, and angle is the angle between the charge concentrations.

electronegative ligands BeH, Li, AlH₂, MgH, and Na. The expected number and arrangement of charge concentrations is not, therefore, observed for ligands less electronegative than carbon, that is, for the molecules that are predominately ionic, and it just for these molecules that the bond angle is substantially larger than the tetrahedral angle.

Why is the VSEPR model apparently not valid unless the ligands are sufficiently electronegative? The basis of the VSEPR model is that, as a consequence of the operation of the Pauli principle, the most probable arrangement of four valence shell electrons with the same spin is at the vertices of a tetrahedron.^{1,37} In an isolated oxide ion, there are a set of four α spin electrons and a set of four β spin electrons, each of which has a most probable tetrahedral arrangement. The two tetrahedra are kept apart by electrostatic repulsion, but neither has a fixed location in space, so the overall electron density of the oxide ion is spherical. However, on combination with a ligand (X^+), one electron of each set is attracted toward the ligand, so that both of these electrons become more localized with a most probable position in the direction of the ligand, thus forming a bonding electron pair. Because each set of same-spin electrons retains its most probable tetrahedral arrangement, each of the other electrons becomes correspondingly more localized, and, in the presence of two or more ligands, four electron pairs with a most probable tetrahedral arrangement are formed. Each electron pair may be said to occupy an electron pair domain centered upon the most probable position of each of the electrons. In the free ion, the domain of each of the electrons may be considered to occupy the whole valence shell; in other words, the electrons are completely delocalized. But in the presence of a sufficiently electronegative ligand, four relatively well localized electron pair domains with a tetrahedral arrangement are formed. However, with decreasing ligand electronegativity, each of the four electron pair domains becomes larger in extent—more spread out or diffuse—and so overlaps its neighbors to an increasing extent until, in the limiting case of an oxide ion, there is no electron localization, and each domain may be considered to occupy the whole of the valence shell.

The localization of pairs of electrons in bonding and nonbonding domains gives rise to an increased electron density in the two bonding and two nonbonding regions. These regions of increased electron density are observed in a relief or contour map of the electron density in the XO₂ plane as ridges

of increased electron density between bonded nuclei or as shoulders of increased density (a bulging out of the contours) in the lone pair directions in the more covalent molecules. In *L*, these shoulders of increased density appear as valence shell CCs and thus become much more evident. It is these concentrations of charge in the tetrahedral directions that determine the geometry of AX_{*n*}E_{*m*} molecules with sufficiently electronegative ligands.

However, with ligands that are less electronegative than carbon, the valence shell electrons of the central atom are not strongly localized and have correspondingly larger domains that have substantial overlap, with the large nonbonding domains overlapping more than the smaller bonding domains. Thus, in (H₂B)₂O, as a consequence of the overlapping of the nonbonding domains, only one nonbonding CC is produced, which forms a triangular arrangement with the two bonding CCs, producing a bond angle of 126.9°. In the linear Li₂O and (HBe)₂O molecules, the oxygen is an almost spherical oxide ion in which the extensively overlapping electron domains give rise to just two collinear bonding CCs separated by a torus of charge depletion. As the localization of the electrons in the valence shell of oxygen decreases, these electrons exert a diminishing effect on the geometry, which is increasingly dominated by electrostatic and/or steric repulsion between the ligands.

In period 3, the change to an angular structure does not occur until silicon, consistent with the electronegativity of silicon (1.7)³⁸ being lower than that of carbon and closer to that of boron. That the bond angle in H₃SiOSiH₃ (148.3°) is somewhat larger than that in H₂BOBH₂ (135.4°), which in turn is slightly larger than that in H₂POPH₂ (129.8°), is consistent with the electronegativity values of Si (1.7), B(2.0), and P(2.1). As in H₂BOBH₂, there is only one nonbonding maximum in the oxygen valence shell in H₂POPH₂ and in H₃SiOSiH₃. As the ligand electronegativity increases, the single lone pair CC separates into two clear maxima in (HS)₂O and Cl₂O. However, because of the lower electronegativity of the ligands in this series, the bond angle does not quite reach the tetrahedral angle, even in Cl₂O. Figure 4 shows that there is a strong correlation between the bond angle for both the period 2 and 3 (H_{*n*}X)₂O molecules and the charge on oxygen. The charge on oxygen reflects the electronegativity of the ligands (Figure 2) and, thus, the extent of the localization of the valence shell electrons, confirming that the bond angle is determined by the degree of localization of the valence shell electrons into bonding and nonbonding pairs.

(37) Linnett, J. W. *The Electronic Structure of Molecules*; Wiley: New York, 1964.

(38) Allred, A. L.; Rochow, E. G. *J. Inorg. Nucl. Chem.* **1958**, *5*, 264.

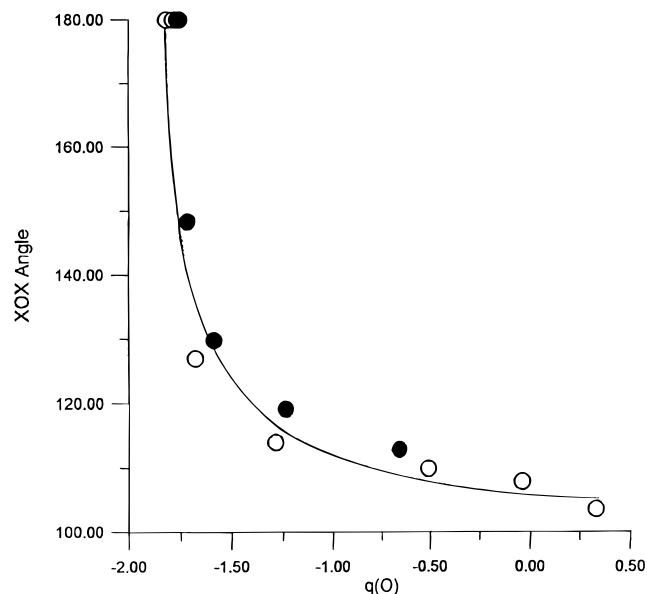


Figure 4. Plot of the XOx bond angle against the charge on oxygen.

The increases localization of the electrons that gives rise to the angular geometry of $(\text{H}_2\text{B})_2\text{O}$ and $(\text{H}_3\text{Si})_2\text{O}$ and the higher members of each series is evident even when the geometry of these molecules is constrained to be linear. In these cases, there is, in addition to two collinear bonding CCs, a toroidal nonbonding charge concentration (see linear $(\text{CH}_3)_2\text{O}$ and $(\text{SiH}_3)_2\text{O}$ in Figure 1) in place of the corresponding region of charge depletion found in molecules such Li_2O and $(\text{HBe})_2\text{O}$, for which the linear geometry has the lowest energy. Because of the linear symmetry of the molecule, the four nonbonding electrons are not constrained to form $\alpha\beta$ pairs; instead, they form a toroidal four-electron domain. This arrangement of charge concentrations has a higher energy than the most probable tetrahedral arrangement, so a molecule that has such a toroidal charge concentration when it has a linear geometry is more stable when it has an angular geometry and a tetrahedral arrangement of four charge concentrations. So $(\text{H}_2\text{B})_2\text{O}$ and $(\text{H}_3\text{Si})_2\text{O}$ and later members of both series have an angular geometry. For these two particular molecules, because the electron localization is relatively weak, the difference in energy between the two geometries is very small, so the energy of linearization is small and the molecules are very floppy. The small linearization energy also accounts for the large range of SiOSi bond angles found in the silicates and other molecules.

Bond Angles and Bond Lengths in Some Related Molecules. The effective electronegativity of the CH_3 and SiH_3 ligands is slightly decreased upon substitution of hydrogen by methyl. Thus, the calculated bond angles at oxygen¹⁷ increase from 125.0° for CH_3OSiH_3 to 127.2° in $\text{H}_3\text{COSi}(\text{CH}_3)_3$ and to 134.4° in $(\text{CH}_3)_3\text{COSiH}_3$, the smaller increase being caused by the less electronegative $\text{Si}(\text{CH}_3)_3$ group.

(i) Digerinoxane ($(\text{GeH}_3)_2\text{O}$). That the bond angle in this molecule (126.5°) is smaller than that in disiloxane and the charge on oxygen (-1.56) is smaller than that on silicon (-1.72), as we see from Tables 1 and 2, is consistent with the greater electronegativity of germanium (2.0) than that of silicon (1.7). Moreover, the bond angle and charge on oxygen in $(\text{GeH}_3)_2\text{O}$ are close to those in $(\text{H}_2\text{P})_2\text{O}$ (129.8° and -1.59), which is consistent with the electronegativity of phosphorus (2.0), which is the same as that of germanium.

(ii) Disilyl Peroxide ($\text{H}_3\text{SiOOSiH}_3$). The SiOO bond angle in $\text{H}_3\text{SiOOSiH}_3$ has been calculated by Oberhammer and Boggs¹⁶ to be 101.2° , quite close to the experimental value of

Table 4. Bond Angles (deg) in SX_2E_2 and OX_2E_2 Molecules

molecule ^a	bond angle	molecule	bond angle
SF_2	98.2	OF_2	103.1
SCl_2	103.0	OCl_2	110.9
$\text{S}(\text{CH}_3)_2$	99.1	$\text{O}(\text{CH}_3)_2$	111.8
$\text{S}(\text{PF}_2)_2$	91.3	$\text{O}(\text{PF}_2)_2$	135.2
$\text{S}(\text{SiH}_3)_2$	98.4	$\text{O}(\text{SiH}_3)_2$	144.1
$\text{S}(\text{CF}_3)_2$	97.3	$\text{O}(\text{CF}_3)_2$	122.2

^a References: SF_2 , Kirchoff, W. H.; Johnson, D. R.; Powell, F. X. *J. Mol. Spectrosc.* **1973**, *48*, 157; SCl_2 , Morino, Y.; Murata, Y.; Ito, T.; Nakamura, J. *Phys. Soc. Jpn.* **1962**, *17(B11)*, 37; $\text{O}(\text{PF}_2)_2$, Yow, H. Y.; Rudolph, R. W.; Bartell, L. J. *J. Mol. Struct.* **1975**, *28*, 20; others, see Table 1.

106.6° for $\text{Me}_3\text{SiOOSiMe}_3$ ³⁹ but much smaller than the SiOSi angle in $\text{H}_3\text{SiOSiH}_3$. These angles are consistent with our suggestion that the bond angles in XOx molecules depend primarily on the electronegativity of the ligand X. Thus, in the series $\text{SiH}_3\text{O}(\text{SiH}_3)$, $\text{SiH}_3\text{O}(\text{CH}_3)$,¹⁶ $\text{SiH}_3\text{O}(\text{OSiH}_3)$, the bond angle decreases from 144.1° to 120.6° to 101.2° with increasing electronegativity of the ligand.

(iii) F_nXOXF_n Molecules. Our conclusion that the short bond lengths and large bond angles in the early members of the H_nXOXH_n series of molecules are due to the large charges on the X and O atoms in these molecules is supported by the effects of fluorine substitution on the bond lengths and angles. Substitution of F for H is expected to increase the charge on the X atom compared to that in the corresponding H_nXOXH_n molecule and, therefore, to decrease the bond length and increase the bond angle. In agreement with this expectation, substitution of F for H increases the bond angle in $\text{H}_3\text{SiOSiH}_3$ from 144.1° to 156° , in H_3COCH_3 from 111.8° to 122.2° , and in H_2POPH_2 from 129.6° (calculated) to 135.2° , while it decreases the bond length in $\text{H}_3\text{SiOSiH}_3$ from 163.4 to 156 pm, in H_3COCH_3 from 141.6 to 135.4 pm, and in H_2POPH_2 from 163.6 to 160.7 pm.

(iv) X_2SE_2 Molecules. Replacing oxygen by sulfur in disiloxane and related molecules would be expected to decrease the bond angle for two reasons: (1) The large size of the sulfur atom increases the distance between the X atoms and, therefore, decreases the repulsion between them. (2) The lower electronegativity of sulfur means that a given ligand X has an electronegativity more comparable to that of sulfur than oxygen, so that the bonds are more covalent and the sulfur valence shell electrons are more strongly localized than the valence shell electrons of oxygen. Table 4 shows that the angles in X_2SE_2 molecules are consistently smaller than those in the corresponding XOx molecules. Because of the greater covalency of the bonds in X_2SE_2 molecules, we expect that the shortening of the bonds would be considerably less than that in the corresponding X_2OE_2 molecules. Again, this prediction is in accord with observations.

(v) AX_3E Molecules. Although AX_3E molecules are not discussed in detail in this paper, the ideas developed here also apply to these molecules, which, according to the VSEPR model, should have a pyramidal geometry. The bond angle increases in the series NF_3 (102.3°),⁴⁰ NH_3 (107.2°),⁴¹ $\text{N}(\text{CH}_3)_3$ (110.9°),⁴² $\text{N}(\text{SiH}_3)$ (120°),⁴³ with decreasing electronegativity of the ligand as the nitrogen valence shell electrons become less localized into pairs. However, when nitrogen is replaced by the consider-

(39) Kaess, D.; Oberhammer, H.; Brandes, D.; Blaschette, A. *J. Mol. Struct.* **1977**, *40*, 65.

(40) Otake, M.; Matsumura, C.; Morino, T. *J. Mol. Spectrosc.* **1968**, *28*, 316.

(41) Helming, P.; de Lucia, F. C.; Goordy, F. W. *J. Mol. Spectrosc.* **1971**, *39*, 94.

(42) Beagely, B.; Medwind, A. R. *J. Mol. Struct.* **1977**, *38*, 229.

(43) Beagely, B.; Conrad, C. *Trans. Faraday Soc.* **1970**, *66*, 2740.

ably less electronegative phosphorus, the bond angles are consistently smaller than those with the corresponding nitrogen molecules, as in $\text{P}(\text{SiH}_3)_3$ (96.8°)⁴³ and $\text{P}(\text{CH}_3)_3$ (98.6°),⁴⁴ for the same reasons as we discussed above for sulfur.

Conclusions

Our results show that it is not necessary to postulate Si–O multiple bonding to explain either the bond angle or the SiO bond length in $\text{H}_3\text{SiOSiH}_3$. The unexpectedly short bond length is a consequence of the considerable ionic character of the SiO bond, as has been suggested previously,¹⁶ and is consistent with similar short bond lengths in related molecules, such as H_2BOBH_2 , in which X is appreciably less electronegative than O, so that the bonds have considerable ionic character. The bond angle in $\text{H}_3\text{SiOSiH}_3$ is consistent with the XOX angles in the series of molecules H_nXOXH_n , where X is a period 2 or a period 3 element, which decrease from 180° to less than the tetrahedral angle with increasing electronegativity of X across the periodic table as the covalent character of the bonds increases and the oxygen valence shell electrons become more localized.

(44) Beagley, B.; Medwind, A. R. *J. Mol. Struct.* **1977**, *38*, 239.

These conclusions are also consistent with those in our recent paper on the nature of the Si–F and related X–F bonds.¹⁹

The VSEPR model is not directly applicable to those molecules in which the electronegativity of the ligand is appreciably less than that of the central atom, in this case oxygen, because the valence shell electrons of the central atom are not sufficiently localized to form the four localized electron pair domains as assumed in the VSEPR model. Nevertheless, the bond angles in disiloxane and other related molecules with weakly electronegative ligands can be understood in terms of the opposing effects of a weak localization of the valence shell electrons of oxygen producing an angular molecule and steric and/or electrostatic repulsions between the ligands that, in the limiting case of a very weakly electronegative ligand such as lithium, lead to a linear geometry.

Acknowledgment. We thank Prof. Richard Bader for the use of his computing facilities and both Prof. Richard Bader and Prof. E. A. Robinson for many helpful discussions and useful comments on earlier drafts of the paper.

IC961381D